Physica Scripta

The Superfluid Transition in Confined ^{4}He: Renormalization-Group Theory

Volker Dohm

Institut für Theoretische Physik, Technische Hochschule Aachen, D-52056 Aachen, Germany

Physica Scripta. Vol. T49, 46–58, 1993

The Superfluid Transition in Confined ^{4}He: Renormalization-Group Theory

Volker Dohm

Institut für Theoretische Physik, Technische Hochschule Aachen, D-52056 Aachen, Germany

Received May 6, 1993; accepted May 16, 1993

Abstract

The present status of the field-theoretic renormalization-group (RG) approach to finite-size effects in ^{4}He near the superfluid transition is reviewed. The perturbation theory is discussed for periodic and Dirichlet boundary conditions. Results of RG calculations of the specific heat, the superfluid density and the thermal resistance near T_λ are presented and compared with experimental data.

1. Introduction

The ideal properties of the superfluid transition of bulk ^{4}He suggest that also confined ^{4}He should be an excellent candidate for testing the theory of static and dynamic finite-size effects near a second-order phase transition of a real system. Of primary importance would be a verification of the finite-size scaling behavior predicted by phenomenological [1] and renormalization-group (RG) theories [2, 3] that has been verified so far only for model systems [4]. Also more detailed investigations such as that of scaling functions, their dependence on realistic boundary conditions (b.c.) and on the geometrical shape of the system as well as the study of dimensional crossover between three and two dimensions are of general interest.

The present situation, however, appears to be unsatisfactory. On the experimental side there seem to exist major difficulties in interpreting previous specific-heat, superfluid-density and thermal-conductivity data of confined ^{4}He near T_λ [5]. And on the theoretical side there exist only very few calculations of scaling properties in the presence of realistic b.c. that can be considered as testable in a fully quantitative sense. There is, however, encouraging agreement between very recent specific-heat data [6] and RG predictions [7, 8] as well as a partially clarifying reexamination [9] of the finite-size scaling problem related to earlier specific-heat data [10–12].

The purpose of this paper is to briefly review the RG theory of finite-size effects in ^{4}He and to discuss part of the existing difficulties. We shall restrict our review to 3-dimensional confinements of regular shape such as cubic and parallel-plate geometry. The interesting but more complex phenomena in ^{4}He confined to random geometries (porous media) [13] will not be discussed. The present review can be considered as complementary to earlier reviews on the RG theory of bulk critical phenomena in ^{4}He [14].

2. Field-theoretic model and finite-size scaling

Consider liquid ^{4}He confined to a finite d dimensional volume V with a characteristic length L. Near the bulk transition temperature T_λ the thermodynamic properties can be derived from the free energy

$$f = f_B - V^{-1} \ln \int D\phi \exp -H, \tag{2.1}$$

where f_B is a background free energy and

$$H = \int_V d^d x [\tfrac{1}{2} r_0 \phi^2 + \tfrac{1}{2}(\nabla\phi)^2 + u_0 \phi^4], \tag{2.2}$$

$$r_0 = r_{0c} + a_0 t,\ t = (T - T_\lambda)/T_\lambda. \tag{2.3}$$

The order-parameter field $\phi(x) = (\phi^{(1)}, \phi^{(2)})$ has two components representing the complex coarse-grained wave function $\psi(x) = \phi^{(1)}(x) + i\phi^{(2)}(x)$ of the Bose condensate. The spatial variations of $\psi(x)$ are cut off at a semi-microscopic length Λ^{-1}. The true boundary conditions for $\psi(x)$ on a mesoscopic length scale are not well established. It is fairly realistic, however, to assume Dirichlet boundary conditions (D.b.c.), i.e. $\psi(x) = 0$, at the solid boundaries [15, 16]. In a more complete description one may add a surface term $c_0 \phi^2$ to (2.2) [17] with a finite (mean field) extrapolation length $c_0^{-1} > 0$. The additional effect of van der Waals forces may also be of some importance [18, 19].

For the purpose of summarizing the general features of the RG theory we first discuss the susceptibility above T_λ

$$\chi(t, L) = \int_V d^d x \langle \phi(x)\phi(0) \rangle \tag{2.4}$$

as an example (although χ is not directly measurable in ^{4}He). In the field-theoretic RG approach [20, 21] the limit $\Lambda \to \infty$ is considered which implies ultraviolet (u.v.) divergencies of χ. In the bulk case and for multiplicatively renormalizable quantities these divergencies can be absorbed by introducing a renormalized field $\phi_R = Z_\phi^{-1/2}\phi$ and the renormalized parameters $r = Z_r^{-1}\ (r_0 - r_{0c})$ and $u = \mu^{-\varepsilon} Z_u^{-1} u_0$, provided that $\varepsilon = 4 - d \geqslant 0$. The reference length μ^{-1} may be conveniently chosen as the amplitude ξ_0 of the asymptotic bulk correlation length

$$\xi = \xi_0 t^{-\nu} \tag{2.5}$$

above T_λ. Since the u.v. divergencies should not depend on the size and on the boundary conditions the same Z factors should suffice to renormalize the susceptibility of a finite (or partially confined) system [3]. This obvious hypothesis has been verified explicitly for periodic b.c. up to two-loop order [22, 23], for D.b.c. up to one-loop order [7, 16, 24], and for various b.c. in film geometry up to two-loop order [25, 26]. As shown by Brezin [3] this implies the finite-size scaling form of the renormalized susceptibility $\chi_R = Z_\phi^{-1}\chi$ and, since

Z_ϕ is independent of t and L, also of the bare (physical) susceptibility $\chi = Z_\phi \chi_R$ itself,

$$\chi(t, L) = \xi^{\gamma/\nu} g_\chi(L/\xi) = L^{\gamma/\nu} f_\chi(L/\xi), \tag{2.6}$$

in the limit $t \ll 1$, $L/\xi_0 \gg 1$. This holds true even at finite Λ provided that $L\Lambda \gg 1$, $\xi\Lambda \gg 1$. Since the bulk exponents γ and ν are accurately known the remaining problem, in the asymptotic region, is to calculate the universal scaling functions such as f_χ. They are "less universal" than γ and ν since they depend on the geometry and the boundary conditions.

It is well known [20, 21] that, besides the multiplicative renormalizations, further additive renormalizations are necessary for important quantities such as the free energy, energy density and specific heat. Not obvious (and not well known), however, is the fact that in contrast to the unmodified bulk Z factors these additive renormalizations have to be changed in case of Dirichlet boundary conditions of the finite system. Then the *constant* bulk subtractions (for example pole terms $\sim (4-d)^{-n}$ in case of the minimal subtraction) are no longer sufficient, as will be discussed in Section 4.2.

The main quantities of interest in confined ^{4}He are the specific heat, the superfluid density and the thermal resistance. Their finite-size scaling behavior analogous to (2.6) as predicted by the RG theory without adjustment of parameters will be discussed in subsequent sections. Also the calculation of nonasymptotic L-dependent deviations are of interest; this does not introduce new nonuniversal parameters since, for ^{4}He, the latter are well known from bulk theory [14, 27] and bulk experiments [28], except for Λ and c_0 mentioned above.

For the purpose of testing the theory and to exhibit the differences between Dirichlet and periodic b.c. it is useful to compare the field-theoretic model also with the 3 dimensional XY model which belongs to the same universality class as ^{4}He. There exist Monte-Carlo (MC) data for cubes of various sizes [29–31]. We call attention, however, to a major difference with ^{4}He: the *sign* of the correction-to-scaling (Wegner [32]) amplitudes. While these amplitudes appear to be positive for ^{4}He (with increasing magnitude at higher pressures [27]) they turn out to be *negative* for the 3d XY model with n.n. interaction as first pointed out in [33–35]. This can be most clearly seen by plotting the MC data of, for example, the susceptibility $\chi(t, L)$ at T_c in the form $\chi(0, L)/L^{\gamma/\nu}$ *vs.* log L (see Section 6). Corresponding nonasymptotic analyses of various bulk and finite-size quantities of spin (Ising, XY, Heisenberg) models have been performed by the Aachen theory group [34, 36, 37] and will be published elsewhere. The negative Wegner amplitudes of the XY model have been confirmed very recently in [38]. From a more fundamental point of view a quantitative description of negative Wegner amplitudes is quite challenging since it requires to take into account a finite cutoff Λ in the field-theoretic RG approach [39].

3. Perturbation approach for periodic b.c.

The mean-field equation $\delta H/\delta\phi = 0$ incorrectly predicts a sharp transition even for a finite system. Correspondingly an expansion around the mean-field solution would be incapable of describing smooth finite-size effects. It was not until 1985 when a systematic perturbation approach was developed [40, 41] for periodic b.c. It is based on the decomposition

$$\phi(x) = \Phi + \sigma(x) \tag{3.1}$$

into the lowest mode

$$\Phi = V^{-1} \int \mathrm{d}^d x \phi(x) \tag{3.2}$$

and the higher modes

$$\sigma(x) = V^{-1} \sum_{k \neq 0} \phi_k \mathrm{e}^{\mathrm{i}kx}. \tag{3.3}$$

Correspondingly (2.2) is decomposed as $H = H_0 + H^1(\Phi, \sigma)$ with

$$H_0 = V(\tfrac{1}{2} r_0 \Phi^2 + u_0 \Phi^4). \tag{3.4}$$

This yields the partition function in the form

$$Z(t, L) = \int_{-\infty}^{\infty} \mathrm{d}^2\Phi \exp - [H_0 + \mathring{\Gamma}(\Phi^2)] \tag{3.5}$$

where

$$\mathring{\Gamma}(\Phi^2) = -\ln \int D\sigma \exp - H^1(\Phi, \sigma) \tag{3.6}$$

contains the contribution of the higher modes. Now, unlike the mean-field order parameter, the lowest-mode average

$$\langle \Phi^2 \rangle_0 = \frac{1}{Z_0} \int \mathrm{d}^2\Phi \Phi^2 \exp - H_0 \tag{3.7}$$

is a smooth function of r_0 at finite V. In this approach only (3.6) is calculated perturbatively whereas the Φ integration in (3.5) is performed (numerically) exactly.

More specifically, (3.6) was treated in [40] by means of an expansion around $\Phi = 0$. This is appropriate for $T \geqslant T_\lambda$ but not for $T < T_\lambda$ [42]. In the approach of [41] the entire exponential $\exp - \mathring{\Gamma}(\Phi^2)$ was expanded around $\langle \Phi^2 \rangle_0$. While this yields results similar to those of [40] for $T \gtrsim T_\lambda$ it creates unphysical features in the temperature dependence below T_λ [42]. A modified perturbation approach that avoids these problems for the case of a one-component order parameter has been developed recently [42]. For a two-component order parameter (as is appropriate for ^{4}He), however, the problem of spurious Goldstone singularities arises for $T < T_\lambda$ at intermediate stages of the calculation [43]. This problem has not yet been solved in a fully satisfactory fashion.

For this reason a new perturbation approach for finite systems is currently under investigation [43] that is based on the decomposition

$$\phi(x) = M_0 + \delta\phi(x). \tag{3.8}$$

Here the smoothly temperature-dependent quantity $M_0 = \langle \Phi^2 \rangle_0^{1/2}$ is defined by (3.7). Equation (3.8) corresponds to the decomposition $\Phi = M_0 + \delta\Phi$ of the lowest-mode amplitude where now $\delta\phi(x) = \delta\Phi + \sigma(x)$ is to be treated perturbatively. Preliminary considerations indicate that this approach is appropriate both above and below T_λ and that it does not suffer from the Goldstone problems mentioned above. It should be extendable also to other boundary conditions.

The approach of [40, 41] was originally introduced within the framework of the ε expansion. It can be incorpor-

ated also in the minimally renormalized theory in 3 dimensions [44–46] as has been done in recent papers [7, 8, 42, 43]. Attempts have been made to study the dimensional crossover from 4-ε to 3-ε dimensions for Ising-like systems above T_c with periodic b.c. [47]. It remains to be seen whether this can be extended to the more difficult (^{4}He) case of a two-component order parameter where Goldstone modes below T_λ, the Kosterlitz-Thouless transition in the limit ($\varepsilon \to 1$) of 2 dimensions and the non-periodic b.c. constitute major problems.

It is straightforward to turn from a cube to a finite rectangular ($L_1 \times L_1 \times L$) box. But for $L_1/L \gg 1$ or $L/L_1 \gg 1$ the lowest mode is no longer well separated from the higher modes, and in the limit $L_1 \to \infty$ (parallel plates) or $L \to \infty$ (cylinder) one encounters the considerably more difficult problem of a lowest-mode continuum instead of a single lowest mode [40]. We shall briefly return to this case in Section 5.3.

4. Perturbation approach for Dirichlet b.c.

Dirichlet b.c. ($\phi = 0$) require a treatment of (2.1) that differs significantly from that for periodic b.c. The main differences are as follows:

(i) In the expansion of $\phi(x)$ into mode functions one must distinguish between $T \gtrsim T_\lambda$ and $T < T_\lambda$ because of the spatial dependence of the order-parameter profile below T_λ.

(ii) Dirichlet b.c. cause surface effects. For $T \gtrsim T_\lambda$ their leading contribution arises from fluctuations at one-loop order whereas for $T < T_\lambda$ they appear already at the mean-field level [22].

(iii) Explicit calculations beyond lowest order, in particular below T_λ, are technically much more difficult than for periodic b.c.

(iv) The renormalization of additively renormalized quantities has to be changed because of $\phi = 0$ boundary effects.

For simplicity we consider a cube ($V = L^d$) with D.b.c. in one (z) direction and p.b.c. in d − 1 (y) directions. (For other cases see Section 5.)

4.1. $T \gtrsim T_\lambda$

Again the decomposition (3.1) is the starting point, but now the lowest mode Φ becomes z dependent,

$$\Phi = \phi_1 \sqrt{2} \sin(\pi z/L), \tag{4.1}$$

and the higher modes

$$\sigma(x) = \sum_{\mathbf{k} \neq 0} \phi_{1\mathbf{k}} \sin(\pi z/L) \exp i\mathbf{k}y + \sum_{n>1} \sum_{\mathbf{k}} \phi_{n\mathbf{k}} \sin(\pi n z/L) \exp i\mathbf{k}y \tag{4.2}$$

contain standing waves with $n \geq 1$. The Hamiltonian is decomposed as $H = H_1 + H^1$ with the lowest-mode part

$$H_1 = V\left[\frac{1}{2}\left(r_0 + \frac{\pi^2}{L^2}\right)\phi_1^2 + \frac{3}{2} u_0 \phi_1^4\right]. \tag{4.3}$$

The higher-mode parts $H^1 = H^{(2)} + H^{(3)} + H^{(4)}$ contain $\phi_{n\mathbf{k}}$ in linear and bilinear, trilinear and quartic form, respectively [22]. The exponent of (3.5) becomes $-H_1 - \tilde{\Gamma}(\phi_1^2)$.

Since H_1 is of the same type as H_0, (3.4), it does not contain a surface contribution which enters only via $\tilde{\Gamma}(\phi_1^2)$. So far this perturbation approach has been applied to the surface energy and specific heat in half-space [22, 48], cubic [7, 8, 16, 49], box [8, 49] and cylindrical [50] geometry. The results are applicable also slightly below T_λ including the maximum of the specific heat.

Equation (4.3) suggests to define a shifted variable [16, 51] $r_0 - r_{0c}(L)$ where

$$r_{0c}(L) = -\pi^2/L^2 + 0(u_0) \tag{4.4}$$

is determined by requiring that the $0(\phi_1^2)$ term of $H_1 + \tilde{\Gamma}$ vanishes at $r_0 = r_{0c}(L)$. In [16] this was explored only incompletely at $0(u_0)$ which seemed to yield $r_{0c}(\infty) - r_{0c}(L) \sim L^{-2}$. As noted in [7] and shown in [49, 52], however, the hypothesis mentioned in Section 2 above implies asymptotically

$$r_{0c}(\infty) - r_{0c}(L) \sim T_\lambda - T_\lambda(L) \sim L^{-1/\nu} \tag{4.5}$$

for sufficiently large L/ξ_0. Thus the introduction of a non-scaling shift of T_λ [16, 53] may be justified for small L but not for large L in a fully renormalized theory with D.b.c.

4.2. *Comment on the additive renormalization*

Not only the bare perturbation approach but also the renormalization procedure requires an important change as compared to periodic b.c. Consider the energy $E = \int d^d x \langle \phi^2 \rangle$. Due to the D.b.c. $\langle \phi^2 \rangle$ is a inhomogeneous (z dependent) quantity that vanishes at the boundaries. This is the origin for the fact that the usual bulk renormalization employing a constant (i.e. z independent) additive renormalization of $\langle \phi^2 \rangle$ is problematic and should be replaced by a z dependent subtraction [48, 54]. As noted by the present author [22] and further discussed in [48, 55] the bulk renormalization removes only the poles (u.v. divergencies) of E at $d = 4$ but not at $d = 3$. The latter arise from divergencies of the renormalized counterpart of $\langle \phi^2 \rangle$ at the boundaries (where the *bare* field $\phi = 0$ is kept fixed) after the energy density has been shifted by an infinite (z-independent) amount in order to subtract the bulk u.v. divergencies. The appearance of these poles at $d = 3$ was overlooked in earlier work using Dirichlet b.c. [24, 56] and was misinterpreted recently [57]. This problem which originates from an incomplete renormalization cannot be convincingly circumvented by first expanding the pole $\sim (d-3)^{-1}$ with respect to $\varepsilon = 4 - d$ and subsequently extrapolating this $0(\varepsilon)$ result to $\varepsilon = 1$. Somewhat surprisingly this point has not found any attention in the standard field-theoretic literature.

4.3. $T < T_\lambda$: *Renormalized mean-field approximation*

The solution ϕ_{MF} of the mean-field equation $\delta H/\delta\phi = 0$ below T_λ with D.b.c. at $z = 0$ and $z = L$ is well known [58]. It is given by $\phi_{MF} = 0$ for $r_0 \geq -\pi^2/L^2$ and

$$\phi_{MF}(z)^2 = (-r_0/4u_0) m(z)^2 \tag{4.6}$$

for $r_0 < -\pi^2/L^2$ where $m(z)$ is determined by an elliptical integral. Although (4.6) incorrectly predicts a sharp transition at $r_0 = -\pi^2/L^2$ it contains reasonably well the physical effect of the suppression of the order-parameter profile well below T_λ caused by the D.b.c. The solution (4.6) can be considered as the lowest-order of a perturbation theory and can be incorporated in a RG treatment which ensures the correct critical exponents [7, 59]. This "renormalized mean-field approximation" (RMFA) provides a semi-quantitative description of the leading deviations from the bulk behavior

due to surface effects [22] and is expected to be applicable to the region $|t| \gtrsim (\xi_0/L)^{1/\nu}$ below T_λ.

4.4. $T \lesssim T_\lambda$: *Renormalized lowest-mode approximation*

A systematic perturbation approach based on the mode functions $\sin(\pi nz/L)$ would lead to an unsolvable multimode problem below T_λ [51] where the order-parameter profile cannot be approximated by a few sinosoidal mode functions. Nevertheless the concept of an expansion of $\phi(x) = \Phi + \sigma(x)$ into modes can be maintained by choosing the lowest mode as [7, 60] $\Phi(z) = \Phi_0 f_0(z)$ where the (appropriately normalized) function $f_0(z)$ is proportional to the mean-field profile $\phi_{MF}(z)$. The basic difference with mean-field theory is the fact that here Φ_0 represents a fluctuating amplitude. After integration over z the lowest-mode Hamiltonian becomes

$$H_0 = V[\tfrac{1}{2}A(r_0, u_0, L)\Phi_0^2 + B(r_0, u_0, L)\Phi_0^4]. \tag{4.7}$$

which replaces H_1, (4.3), and joins H_1 smoothly at $r_0 = -\pi^2/L^2$. The complete expressions for A and B are given in [59]. They have the appropriate bulk ($L \to \infty$) limits r_0 and u_0. Neglecting higher modes the free energy is calculated as

$$f_0 = f_B - V^{-1} \ln \int d^2\Phi_0 \exp -H_0. \tag{4.8}$$

This approximation can be incorporated in a RG treatment which ensures the correct critical exponents and is appliable to the entire region $T \lesssim T_\lambda$.

In principle this approach can be made systematic by expanding $\sigma(x) = \sum_{\lambda \neq 0} \Phi_\lambda f_\lambda(x)$ into mode functions $f_\lambda(x)$ whose z dependence is determined by the eigenfunctions of the operator [60]

$$-\frac{d^2}{dz^2} + r_0 + 12u_0\langle\Phi_0^2\rangle_0 f_0(z)^2. \tag{4.9}$$

It can be shown [59] that $f_\lambda(x)$ including $f_0(z)$ constitute a complete orthonormal set of eigenfunctions of (4.9) and that the smallest eigenvalue is associated with $f_0(z)$. In practice, however, it will be hard to go beyond the "renormalized lowest-mode approximation" (RLMA) defined by (4.7) and (4.8).

5. Specific heat of confined ^{4}He

Within the model (2.2) the specific heat of confined ^{4}He (at given temperature, volume, and chemical potential [61]) is defined by

$$C(t, L) = C_B + \frac{a_0^2}{V}\frac{\partial^2}{\partial r_0^2} \ln \int D\phi \exp -H \tag{5.1}$$

where C_B is a noncritical background contribution. This quantity is the most favorable candidate for detailed quantitative tests of finite-size theory without adjustment of parameters. All nonuniversal parameters are already known from comparison between bulk theory [14, 27] and bulk data [28]. RG calculations of $C(t, L)$ for periodic and Dirichlet b.c. have been performed for different geometries in 3 dimensions [7, 8, 16, 22, 42, 43, 50, 52, 55] and in $4 - \varepsilon$ dimensions [25, 26, 41].

5.1. *Periodic b.c.*

Recent quantitative RG calculations in 3 dimensions [34, 43] of $C(t, L)$ for a cube with periodic b.c. predict two general features:

(i) The height of the specific-heat maximum at $T_m < T_\lambda$ is smaller than the bulk value at T_m.

(iii) $C(t, L)$ crosses the bulk curve only once for $t \gtrsim 0$ and approaches the bulk curve from above for $t > 0$.

This is illustrated in Fig. 1. These features are consistent with MC data for the $3 - d$ XY model [29–31]. Furthermore the RG calculations confirm the expectation [1] that finite-size effects set in at temperatures t where $\xi(|t|) \approx 0(L)$. We note that it is only the modified perturbation approach [42, 43] mentioned in Section 3 that correctly yields the properties (i) and (ii). The method of [41] incorrectly predicts a maximum of $C(t, L)$ whose height is larger than the bulk specific heat at T_m; as a consequence $C(t, L)$ crosses the bulk curve three times as shown in Fig. 1(a) of [16] and in Fig. 1(a) of [7] where the method of [41] was employed. We also note that the scaling function in Fig. 4 of [41] contains an unphysical dip below T_m that is not present in the MC data and in the theory of [42, 43].

5.2. *Dirichlet b.c. in two directions*

The effect of Dirichlet b.c. on the finite-size critical behavior of the specific heat was first studied in [16]. As general results it was found

(i) that the suppression of the order parameter at the boundaries ($\psi = 0$) implies that $C(t, L)$ is smaller than $C(t, \infty)$ for any t, in contrast to periodic b.c., (see Fig. 1),

(ii) that surface effects cause $C(t, L)$ to deviate *gradually* from $C(t, \infty)$ much farther from T_λ than in case of periodic b.c., i.e. these effects set in at temperatures t where $\xi(|t|) \ll L$.

For simplicity the experimental situation [11, 12] (pore geometry of diameter L) was modeled by a cube of length L with Dirichlet b.c. in two directions and periodic b.c. in the remaining one. The RG calculation was carried out [16, 50] within an approximation that takes into account the bilinear contribution $H^{(2)}$ of the higher-mode part of the Hamiltonian.

Quantitative results of the RG calculation of $C(t, L)$ (including nonuniversal effects) [16, 50] are shown in Figs. 2–4 for several L. For comparison the result for periodic b.c.

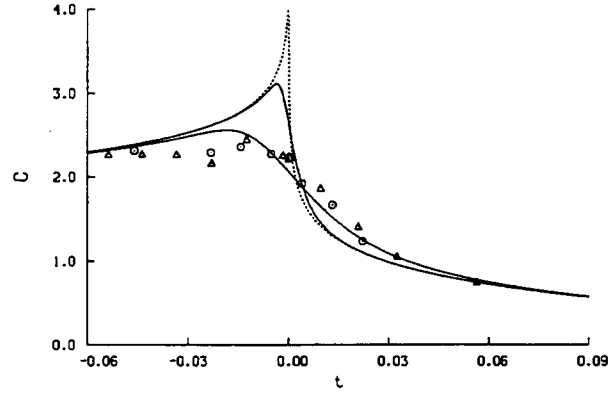

Fig. 1. Specific heat of the ($L \times L \times L$) XY model with periodic b.c. MC data for $L = 16$ (in units of the lattice spacing) from [29–31]. Field-theoretic predictions for $L = 16$, $L = 48$ (solid lines) and $L = \infty$ (dotted line) from [34, 43].

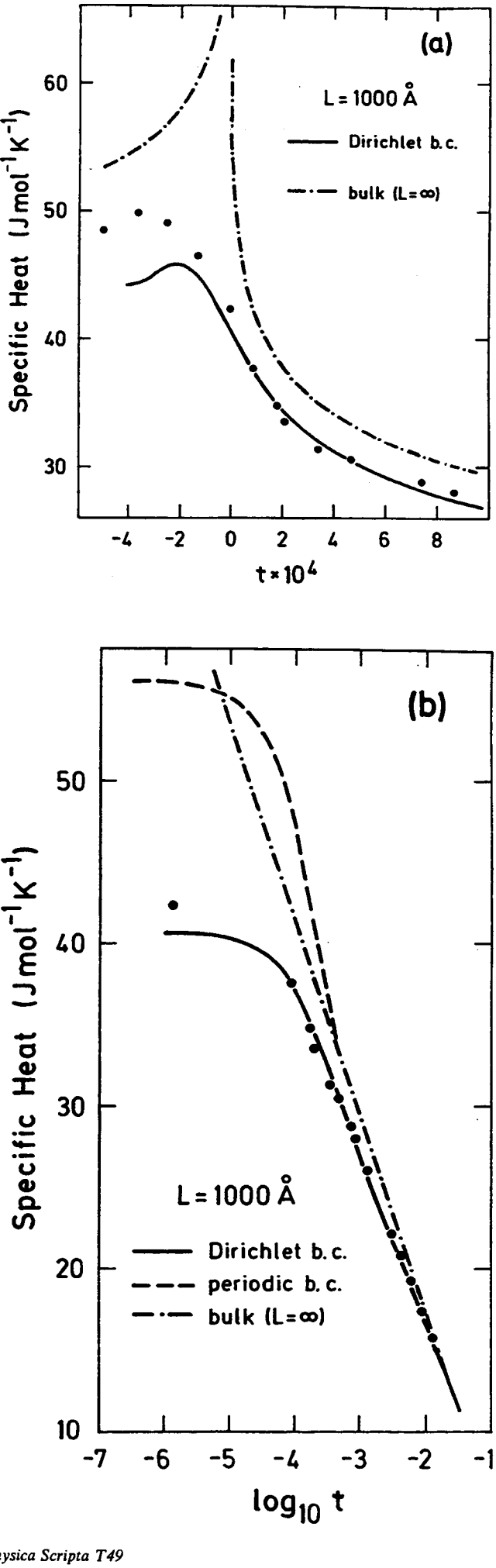

Fig. 2. Theoretical specific heat [16] (solid lines) of ^{4}He confined to a cube ($L = 1000$ Å) with D.b.c. in 2 directions and p.b.c. in one direction *vs.* $t = (T - T_\lambda)/T_\lambda$ (a) and $\log_{10} t$ (b). Data for cylindrical pores of diameter $L = 1000$ Å from [10, 11]. Dashed line: cube with p.b.c. in all directions. Dot-dashed line: bulk.

for the case $L = 1000$ Å is also shown. The reduction of the specific-heat (as compared to that for periodic b.c.) and the algebraic (rather than exponential) approach of $C(t, L)$ for $t > 0$ towards the bulk curve from *below* are well confirmed by the pore data. These features do not sensitively depend on the choice of the reference temperature, e.g. bulk T_λ or a shifted $T_c(L) < T_\lambda$ (the latter, however, was chosen inadequately in [16], see Section 4.1). The overall agreement with the data supports the assumption $\psi = 0$ near the walls (but does not exclude the possible relevance of additional surface effects on a more refined level).

In Fig. 4 the nonuniversal pressure dependence at $L = 1\,\mu$m is predicted [50]. Preliminary results were also obtained by Huhn [50] for the much more difficult case of cylindrical geometry (infinite extension in the z direction) which involves a lowest-mode continuum.

A diagrammatic perturbation approach [22] permits to systematically include the higher-order interactions $H^{(3)}$ and $H^{(4)}$. A complete one-loop calculation using this approach for the case of a cube with Dirichlet b.c. in one direction [49] confirmed the features (i) and (ii) noted above and did not yield significant differences compared with the simpler calculation [16] based on $H^{(2)}$.

5.3. *Dirichlet b.c. in one direction*

Confining ^{4}He between two parallel plates of distance L is the most favorable geometry for an experimental study of $C(t, L)$. Corresponding specific-heat data for $L = 19\,\mu$m have been recently presented [6] and further measurements are in preparation [62, 63]. From a theoretical point of view, however, this plate geometry poses problems below (bulk) T_λ where the effects of the Kosterlitz-Thouless transition at $T_{KT} < T_\lambda$ are present. An additional difficulty is the continuum of wave vectors $\mathbf{k}$ in the mode expansion

$$\phi(\mathbf{y}, z) = \sum_{n=1}^{\infty} \int_k \mathrm{d}^{d-1}k \phi_{nk} \sin(\pi n z/L) \exp i\mathbf{k}\mathbf{y}. \tag{5.2}$$

Recently [25, 26] this expansion was employed in a perturbation theory with respect to the $u_0 \phi^4$ term of (2.2). The resulting $C(t, L)$ is applicable to $T \gtrsim T_\lambda$ and slightly below T_λ for finite L but not to the maximum of C below T_λ. In the spirit of [40] and [41], one would like to proceed by decomposing ϕ into a (non-perturbatively treated) lowest-mode continuum $\sim \phi_{1\mathbf{k}}$ plus higher (perturbatively treated) modes. Presumably this approach, if feasible, would permit to describe reasonably well the finite maximum of $C(t, L)$ below T_λ at finite L even if the Kosterlitz-Thouless-type contributions are not yet included. The calculations in [25, 26] were performed in $4 - \varepsilon$ dimensions. The results appear to suffer from considerable ambiguities regarding the extrapolation to $\varepsilon = 1$. A calculation directly in 3 dimension within the concept of [44–46] is performed in [8, 55]. Some results are presented in Figs. 5–8.

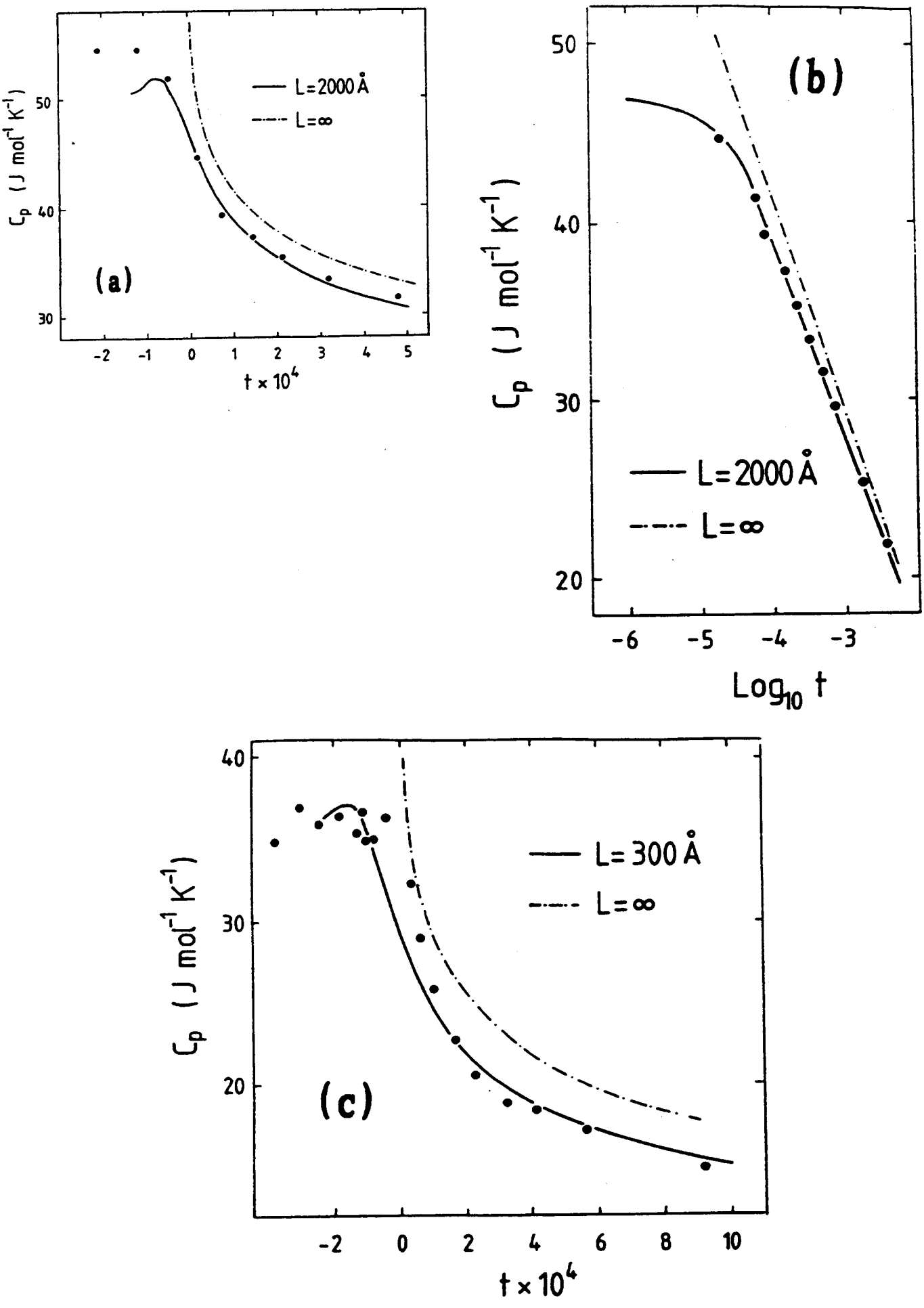

Fig. 3. Theoretical specific heat (solid lines) [50] as in Fig. 2 for $L = 2000$ Å (a, b) and $L = 300$ Å (c). Data from [10, 11].

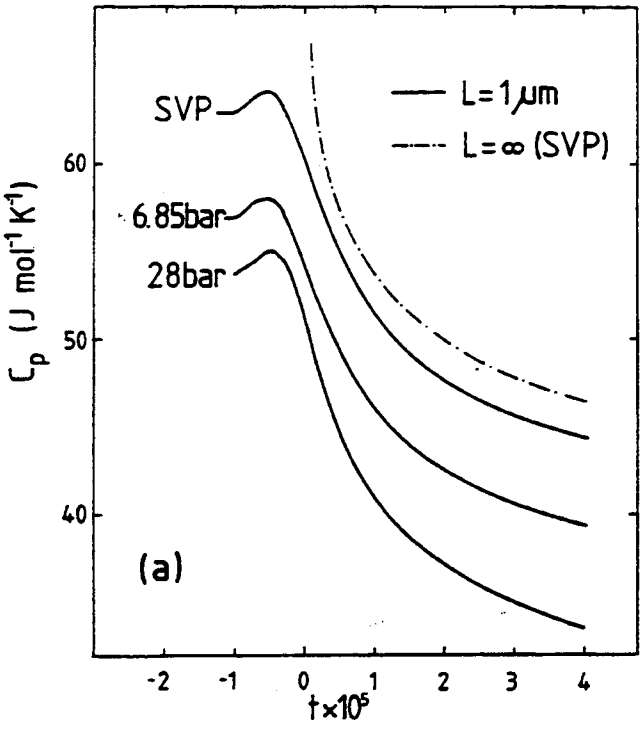

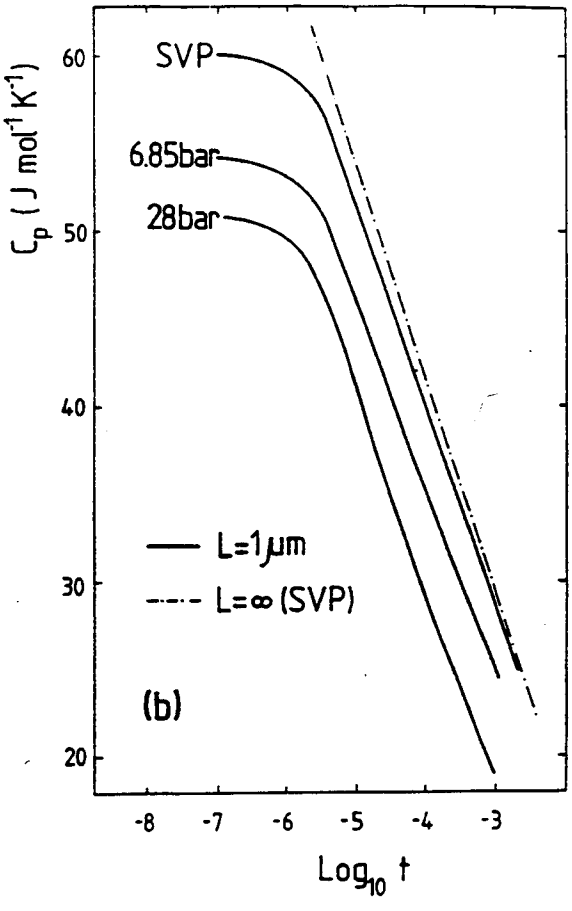

Fig. 4. Theoretical specific heat [50] as in Figs. 1 and 2 for $L = 1\,\mu$m predicted for SVP, 6.85 bar and 28 bar.

Well above T_λ, in the range where $\xi \lesssim L$, the first deviation of $C(t, L)$ from the 3 dimensional bulk behavior may be modeled by a rectangular $(L_1 \times L_1 \times L)$ box with periodic b.c. in two (L_1) directions and Dirichlet b.c. in one (L) direction. The plate geometry corresponds to $L_1 \gg L$. For comparison also the cubic case $L_1 = L$ is of interest.

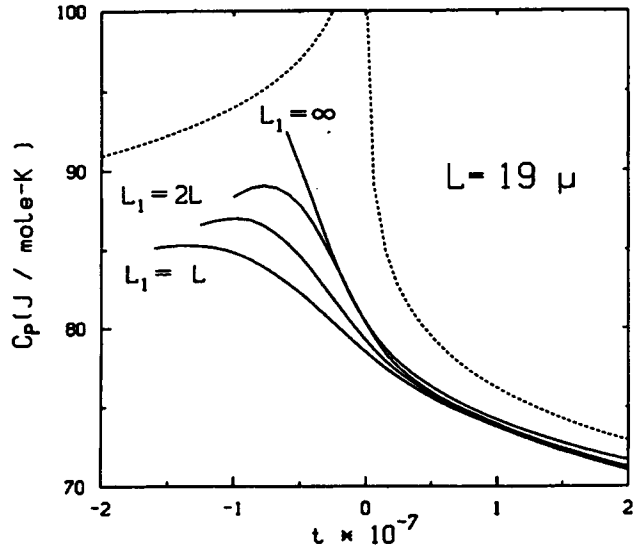

Fig. 5. Theoretical specific heat of ^{4}He confined to a $(L_1 \times L_1 \times L)$ box with D.b.c. in one (L) direction for $L_1 = L$ (cube), $L_1 = 1.3L$, $L_1 = 2L$, and $L_1 = \infty$ (parallel plates) at $L = 19\,\mu$m. Dotted lines: bulk. From [8].

[The corresponding results above and below T_λ will be presented in general scaling forms in Section 5.4]. By varying L_1 one can study the geometrical crossover from cubic to plate geometry. The results of the $d = 3$ RG calculations of $C(t, L)$ in cubic, box, and plate geometry are compared in Fig. 5 for the example $L = 19\,\mu$m [8]. We see that the effect due to different geometric shapes is weak for $T \gtrsim T_\lambda$ but strong near the maximum of C below T_λ. The result for plate geometry is compared with recent data [6] in Fig. 6. In Fig. 7 the specific heat at T_λ for plate geometry is shown as obtained from the $d = 3$ (solid line) and the $4 - \varepsilon$ (dotted line) [26] calculations. For comparison the data of [10–12] and [6] at $T \approx T_\lambda$ are also shown. The agreement of the $d = 3$ theory with the data is encouraging and supports the conclusion [16] that Dirichlet b.c. at solid walls are fairly

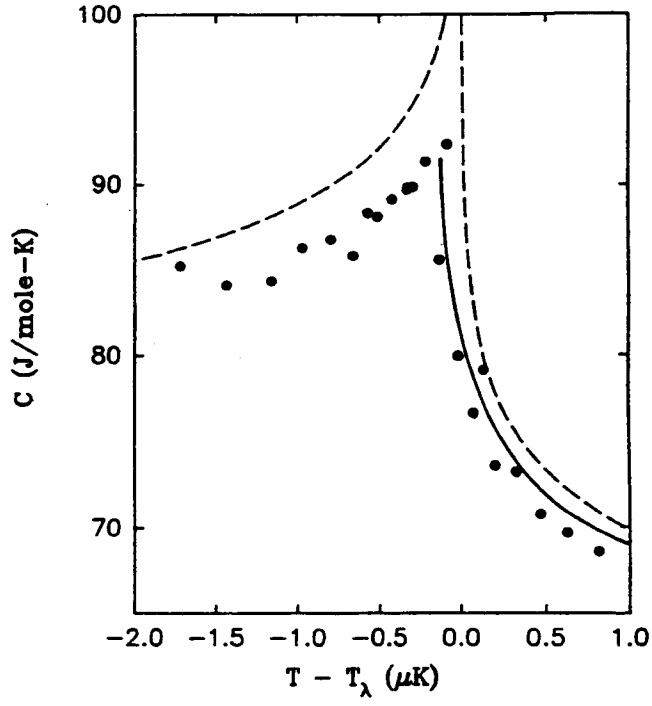

Fig. 6. Theoretical specific heat (solid line) [8] as in Fig. 5 and data [6] for plate geometry at $L = 19\,\mu$m. Dashed lines: bulk.

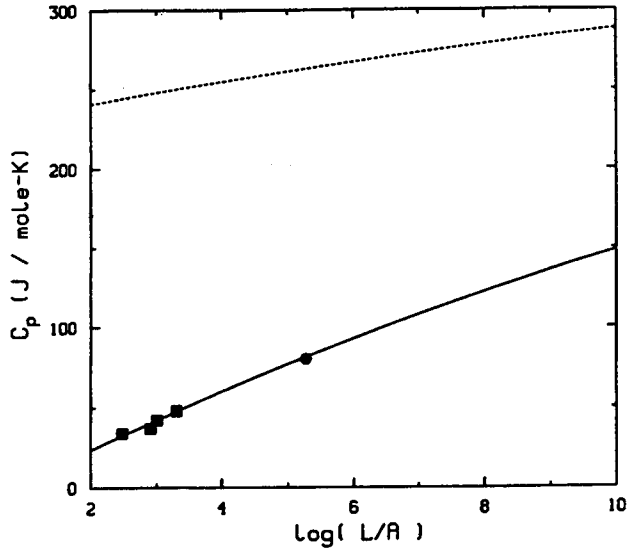

Fig. 7. Specific heat at T_λ *vs.* $\log_{10} L$ for plate geometry. Predictions of field theory in $d = 3$ dimensions [8] (solid line) and in $d = 4 - \varepsilon$ dimensions extrapolated to $\varepsilon = 1$ [26] (dotted line). Data from [10, 11] (squares) and from [6] (circle). From [8].

realistic. In Fig. 8 we also show predictions of $C(t, L)$ for plates at larger distances [8] as is appropriate for planned experiments [62] under microgravity conditions which permit to test finite-size scaling at macroscopic distances L.

5.4. *Scaling functions*

From the hypothesis mentioned in Section 2 it follows [3] that asymptotically ($|t| \to 0$, $L \to \infty$) the difference

$$C(t, L) - C(t, \infty) = |t|^{-\alpha} g(tL^{1/\nu}) \tag{5.3}$$

has a scaling form, analogous to (2.6). This implies that the position $T_m(L)$ of the specific-heat maximum satisfies asymptotically

$$T_\lambda - T_m(L) \sim L^{-1/\nu}. \tag{5.4}$$

The scaling function $g(x)$ is singular at $x = 0$ and is quite sensitive to differences in the representation of $C(t, \infty)$ $= (A^{\pm}/\alpha)|t|^{-\alpha} + B$ [64]. An alternative representation of (5.3) is [7]

$$C(t, L) - C(t_0, \infty) = L^{\alpha/\nu} f_1(tL^{1/\nu}) \tag{5.5}$$

where $t_0 = (\xi_0/L)^{1/\nu}$ is the reduced temperature at which $\xi = L$. The scaling function $f_1(x)$ has the advantage of being smooth and finite at $x = 0$. Furthermore, the representation [7]

$$C(t, L) - C(t, \infty) = -L^{\alpha/\nu} f_2(tL^{1/\nu}) \tag{5.6}$$

is useful since for $x \gg 1$ the scaling function $f_2(x) \sim x^{-\alpha-\nu}$ exhibits the exponent $\alpha_s = \alpha + \nu$ of the surface specific heat $C_s \sim L^{-1} t^{-\alpha_s}$. The shape of these scaling functions for various geometries and boundary conditions as predicted by the RG theory can be inferred directly from the previous curves for $C(t, L)$ in Figs 1–8.

For the example of a cube with Dirichlet b.c. in one direction the one-loop scaling functions $f_1(x)$ and $f_2(x)$ for $x \gtrsim 0$ are shown in Figs 9(a) and 10 [7]. For $x < 0$ ($T < T_\lambda$), $f_1(x)$ was calculated [7] by means of both the RLMA of Section 4.4 (solid line) and the RMFA of Sect. 4.3 (dotted line) [Fig. 9(b)]. The dotted line in Fig. 10 is the surface specific heat $C_s \sim t^{-\alpha-\nu}/L$. Note that the pure surface exponent $\alpha_s = \alpha + \nu$ is exhibited by $f_2(x)$ only for $x \gtrsim 200$, i.e. only for sufficiently large L in the asymptotic range $t < 10^{-2}$. Otherwise only an effective exponent $\alpha_s^{\text{eff}}(x) < \alpha_s$ is seen (solid line in Fig. 10). This holds true also for D.b.c. in two directions and is therefore important for the following analysis.

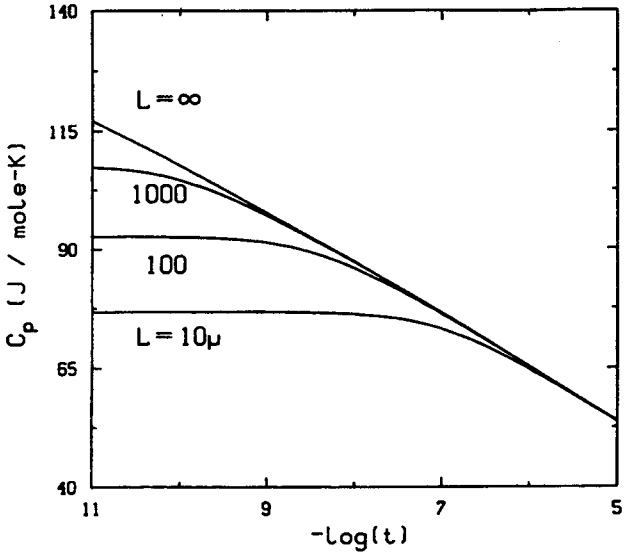

Fig. 8. Theoretical RG prediction [8] of the specific heat of ^4He confined between parallel plates at distance $L = 10$, 100, and 1000 μm for $t > 0$.

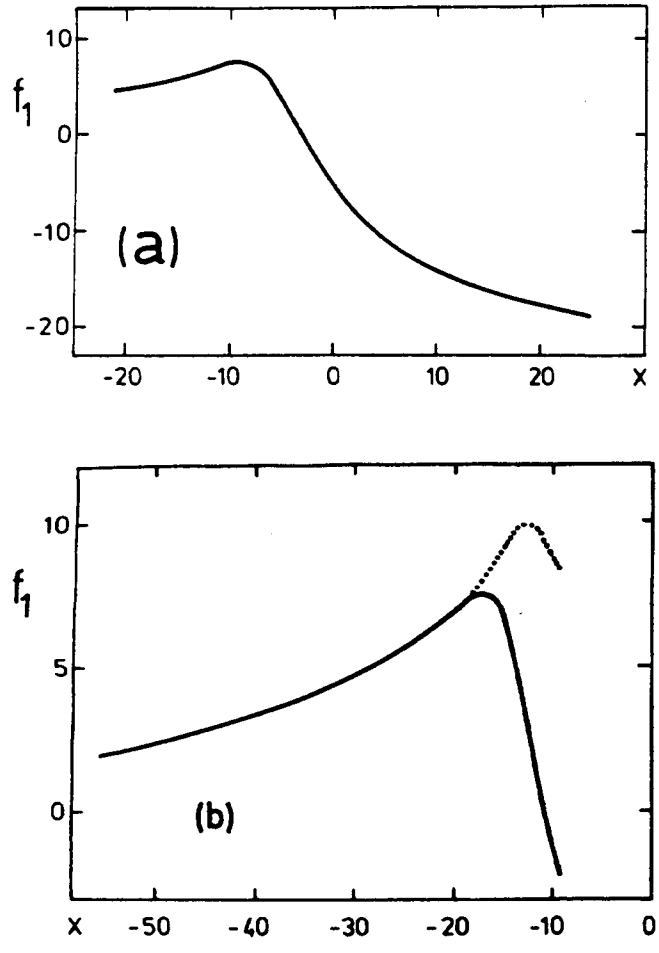

Fig. 9. Scaling function $f_1(x)$, $x = tL^{1/\nu}$, with L in Å, as defined in (5.5), for a cube with D.b.c. in one direction for $t \gtrsim 0$ (a) and $t \lesssim 0$ (b). From [7].

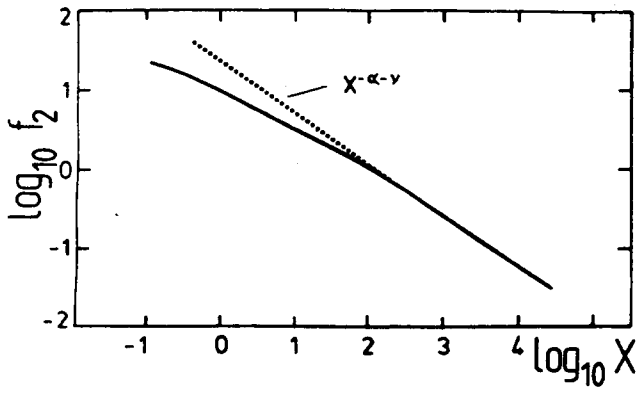

Fig. 10. Scaling function $f_2(x)$, $x = tL^{1/\nu}$, with L in Å, as defined in (5.6), for a cube with D.b.c. in one direction for $t > 0$. The dotted line is the surface specific heat $C_s \sim t^{-\alpha-\nu}/L$. From [7].

5.5. *New analysis of specific-heat data*

In discussing the scaling properties of previous specific-heat data convincing reasons have been given in Section 4 of Ref. [5] to focus on the data [10] of ^{4}He confined to pores of diameter $L = 300 - 2000$ Å. The previous analyses [5, 11, 12] appeared to reveal two major discrepancies with the scaling predictions:

(i) The specific-heat maxima yielded the power law (5.4) with the exponent $\nu = 0.58$ rather than the bulk value $\nu = 0.67$.

(ii) The analysis in terms of the representation $[C(t, L) - C(t, \infty)] \cdot L \sim t^{-\alpha_s}$ yielded a surface exponent $\alpha_s = 0.44$ instead of $\alpha_s = \alpha + \nu = 0.66$.

In [16] a possible explanation of the discrepancy (i) was offered in terms of a correction term $\sim L^{-2}$ arising from a nonscaling shift $T_\lambda - T_c(L) \sim L^{-2}$ of a size-dependent reference temperature $T_c(L)$. As noted in [7] and in Section 4 above, however, this explanation is not consistent at large L/ξ_0 with a fully renormalized theory.

Subsequently a new data analysis based on the original data [10] was carried out for $T \gtrsim T_\lambda$ [49] and $T \lesssim T_\lambda$ [59]. The main results for $T \gtrsim T_\lambda$ have been recently presented in [9]. It turns out that, within realistic error bars of the data, there is no contradiction to finite-size scaling. The earlier dscrepancy (i) was apparently due to the use of specific-heat maxima whose values and error bars [12] were not in agreement with the original data of [10]. By contrast, the recent analysis [9, 52] is well consistent with (5.4) with $\nu = 0.67$ as is demonstrated in Fig. 11. Furthermore, the earlier discrepancy (ii) was presumably due to a misinterpretation [12] of the observed effective surface exponent $\alpha_s^{\text{eff}} < \alpha_s$; as demonstrated by Fig. 10 the pure α_s itself is not observable in the range $L \leqslant 2000$ Å (under the restriction $t < 10^{-2}$ since for $t > 10^{-2}$ nonasymptotic effects would mask the exponent α_s). Thus there is no contradiction to finite-size scaling; one must admit, on the other hand, that the pore data [10–12] are not sufficiently accurate to provide a confirmation of finite-size scaling either.

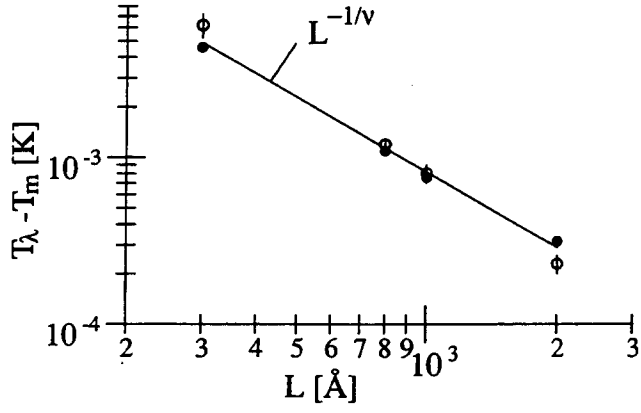

Fig. 11. Shift $T_\lambda - T_m(L)$ of the specific-heat maxima of the data of [10] *vs.* L in a double-logarithmic plot. Open circles with error bars from the earlier analysis of [11, 12]. Full circles from a new analysis [9, 52]. The solid line has the scaling slope $-1/\nu$ which is consistent with the solid circles. From [9].

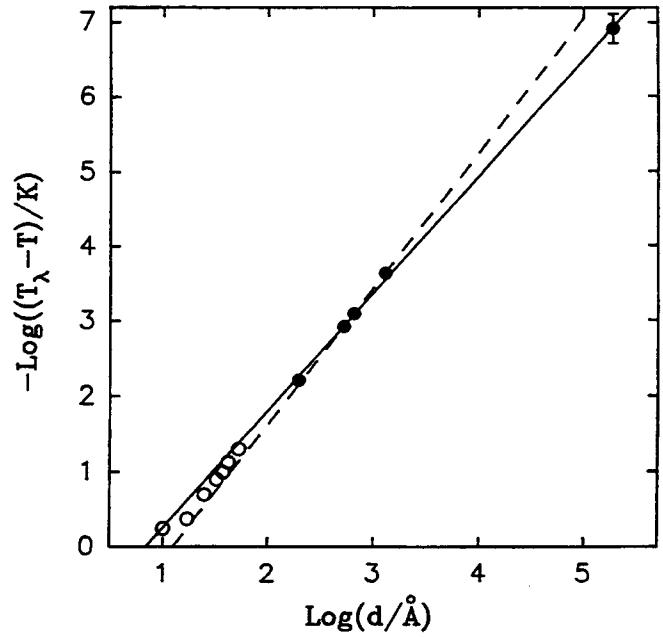

Fig. 12. Shift $T_\lambda - T_m$ of the specific-heat maxima as presented in Fig. 5 of [6]. Open circles: from film data of [10, 11]. Solid circles: from the earlier analysis of the pore data [10] as presented in [5, 11, 12] corresponding to the open circles in Fig. 11. Upper solid circle (with error bar) from [6]. The slope of the solid line is consistent with scaling, the dashed line corresponds to the analysis of [11, 12].

The new specific-heat data shown in Fig. 6, however, and the data analysis by the authors of [6], together with the agreement with the RG results [7, 8], provide significant support for (but do not yet prove) the validity of finite-size scaling of the ^{4}He specific heat. This is substantiated in particular by Fig. 12 which complements and extends the scaling line $\sim L^{-1/\nu}$ of Fig. 11 by two orders of magnitude in L. Nevertheless further measurements at large L [62, 63], preferably under microgravity conditions, are highly desirable to provide more stringent tests of finite-size scaling and to examine the surface exponent α_s.

6. Superfluid density of confined ^{4}He

At present there exist fundamental difficulties in reconciling finite-size theory with the available data of the superfluid density $\rho_s(t, L)$ of confined ^{4}He. For a detailed review on this problem we refer to [5].

Phenomenological scaling theory [1] and general RG arguments parallel to those of Section 2 predict the asymptotic scaling form for the superfluid fraction

$$\frac{\rho_s(t, L)}{\rho} = |t|^\nu g_\rho(|t| L^{1/\nu}). \tag{6.1}$$

Alternatively this may be written as

$$\left[\frac{\rho_s(t,\infty)}{\rho} - \frac{\rho_s(t,L)}{\rho}\right]|t|^{-\nu} = f_\rho(|t|L^{1/\nu}). \tag{6.2}$$

A precise theoretical definition of $\rho_s(t, L)$ is not straightforward. We recall that the bulk ρ_s can be defined in terms of the transverse order-parameter correlation function [65, 66], in terms of the helicity modulus [67], or via the (mass) current-current correlation function [66, 68]. It is not obvious which of these (or other static) bulk definitions is most adequate to describe ρ_s of confined ^{4}He, in particular in view of the fact that $\rho_s(t, L)$ has been measured by means of dynamic experiments [5].

At the present level of the RG calculations [7, 59] of the scaling function (6.2), however, these differences in defining ρ_s do not yet come into play. These low-order calculations of f_ρ have been performed on the basis of the model of Section 2 using the RMFA and RLMA of Section 4.3 and 4.4. For a cube with D.b.c. in one direction the result is shown in Fig. 13 where $\rho_s(t, \infty)/\rho = k|t|^\nu$ with $k = 2.35$ was used. By contrast, the data of [69] plotted in the same way do not collapse on a single scaling curve. This problem is as yet unresolved.

An attempt has been made to explain part of the discrepancy in terms of van der Waals forces [19]. Furthermore it has been suggested [70] that there exists a nonscaling (logarithmic) L dependence of $\rho_s(t, L)$. The corresponding fit [71] to the data, however, is not encouraging. According to a very recent calculation of the helicity modulus within the mean spherical model [72] there exists no logarithmic term of the type suggested earlier [70]. On the other hand MC studies of the XY model [73] appear to be consistent with a logarithmic term. Apparently the problems mentioned so far do not show up in the finite-size scaling analysis of path-integral simulations of the superfluid transition [74].

It may be useful to test the finite-size RG theory below T_λ in more detail for the simpler case of periodic b.c. before more ambitious calculations with realistic b.c. are carried out. For this purpose the comparison with MC data of the

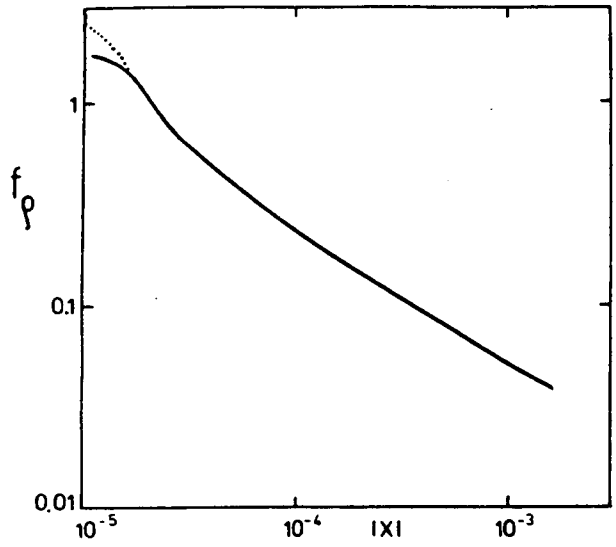

Fig. 13. RG result for the scaling function (6.2) of the superfluid density *vs.* $|x| = |t|L^{1/\nu}$, L in Å, for a cube with D.b.c. in one direction. Solid line: RLMA. Dotted line: RMFA. From [7]. The same scaling plot is employed for the data in Fig. 4 of [69].

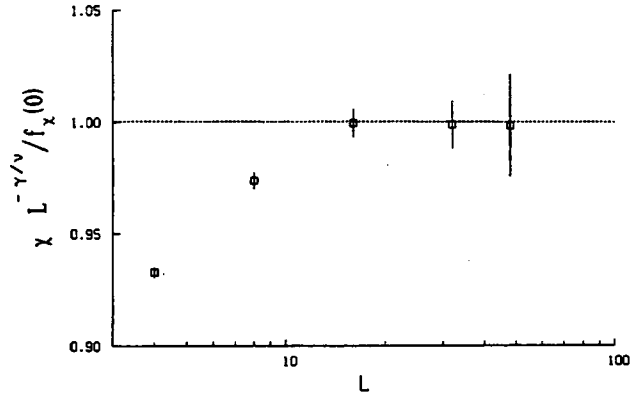

Fig. 14. MC data (with error bars) of [29] of the susceptibility of the XY model at T_c plotted according to (6.3) [33–35]. The data for $L < 10$ (units of the lattice constant) indicate a negative Wegner amplitude.

XY model are helpful. In this context we take up our remark in Section 2 concerning the different signs of the Wegner amplitudes of ^{4}He and of the XY model. In order to identify the leading nonasymptotic corrections we have plotted in Fig. 14 the MC data [29] for the susceptibility at T_c of the 3-*d* XY model (with p.b.c.) in the form

$$\frac{\chi(0, L)}{L^{\gamma/\nu} f_\chi(0)} = 1 + \tilde{a}_\chi (L/\xi_0)^{-\omega} + \cdots, \tag{6.3}$$

compare (2.6), where the r.h.s. exhibits the leading correction term. The MC data approach the asymptotic ($L \to \infty$) value 1 from *below*, thus indicating a negative Wegner amplitude $\tilde{a}_\chi$ of the XY model, in contrast to real ^{4}He [27], but similar to Ising [33, 37] and Heisenberg [35, 43] models.

7. Thermal resistance of confined ^{4}He

It has been suggested [14, 22, 75] that the thermal conductivity or the thermal resistance of confined ^{4}He is the best candidate for testing the theory of dynamic finite-size and surface effects in a real system. This is due to the well observable critical effect arising from the reversible coupling g_0 in the equations of motion (see below) which causes the bulk thermal conductivity and the surface (Kapitza) resistance to diverge at T_λ. Furthermore, below T_λ, superfluid ^{4}He provides a unique opportunity of studying pure dynamic surface properties as *leading effects* because the thermal bulk resistance vanishes exactly (in the absence of vortices in the limit of a vanishing heat current).

More specifically, let us consider ^{4}He in a cell of finite thickness L (plate geometry) with a temperature difference $\Delta T = T_1 - T_2$ across the cell in the presence of a finite stationary heat current Q. Then the total thermal resistance

$$R^{\text{tot}} = \frac{\Delta T}{Q} \tag{7.1}$$

can be decomposed as

$$R^{\text{tot}} = R + \tilde{R}_K^{(1)} + \tilde{R}_K^{(2)} \tag{7.2}$$

where R results *solely from the* ^{4}He *liquid*. The last two terms $\tilde{R}_K$ in (7.2) are the (noncritical) Kapitza resistance of the two solid surfaces. In the linear-response regime ($Q \to 0$), the ^{4}He contribution $R(t, L)$ can be sketched schematically [48, 75] as shown in Fig. 15. The ordinary bulk thermal

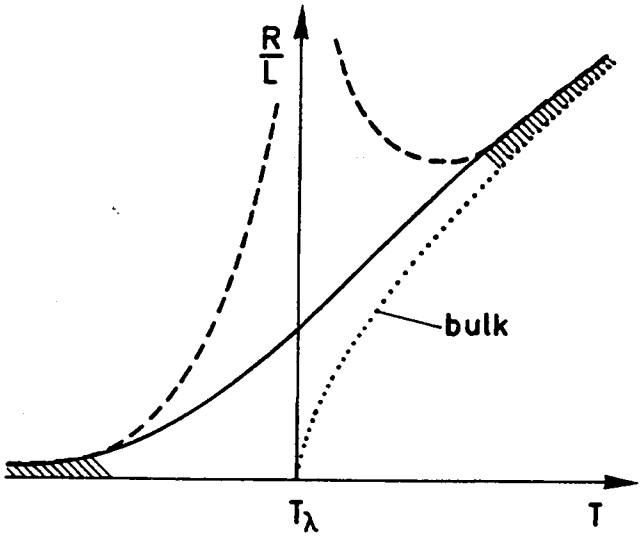

Fig. 15. Schematic plot of the ^{4}He part of the thermal resistance $R(t, T)$ (solid line) of a finite cell of thickness L in the linear-response limit $Q \to 0$. The dashed areas indicate the gradual onset of surface effects and the dashed lines represent $(R_b + R_K^{(1)} + R_K^{(2)})/L$ schematically, with divergent surface contributions R_K. The dotted line represents the inverse bulk thermal conductivity $\lambda_T^{-1} = R_b/L$ above T_λ. Finite-size effects imply a smooth T dependence (solid line) and a finite value of R/L at T_λ. From [48, 75].

conductivity is defined as

$$\lambda_T(t) = \lim_{L\to\infty} L/R(t, L). \tag{7.3}$$

Critical surface contributions $R_K(t)$ to

$$R(t, L) = \frac{L}{\lambda_T(t)} + (R_K^{(1)} + R_K^{(2)})\{1 + 0(\xi/L)\} \tag{7.4}$$

arise from the layer of liquid ^{4}He near the solid walls where the fluctuations of the order parameter are suppressed because of the D.b.c. The surface effects set in gradually as T_λ is approached, and finite-size effects imply a smooth temperature dependence of $R(t, L)$ across T_λ (Fig. 15). From scaling arguments one obtains at T_λ

$$R(0, L)/L \sim L^{-x_\lambda/\nu} \tag{7.5}$$

where x_λ is the effective exponent of the bulk thermal conductivity $\lambda_T(t) \sim t^{-x_\lambda}$. No prediction of the amplitude in (7.5) is as yet available. A corresponding RG calculation is planned for future research.

These considerations should be generalized to the (experimental) situation where a finite Q is present. We may still decompose

$$R = R_b + R_K^{(1)} + R_K^{(2)} + \Delta R \tag{7.6}$$

into bulk, surface (Kapitza) and finite-size contributions where R_b is supposed to be proportional to L, R_K is independent of L, and ΔR is the remaining finite-size part. The finite-Q effects further suppress the effective thermal conductivity [76], i.e. they enhance the thermal resistance, and one may observe combined finite-size, surface and/or nonlinear-Q effects, depending on ΔT and on the ratio L/ξ_Q where

$$\xi_Q = (g_0 k_B T_\lambda/Q)^{1/(d-1)} \tag{7.7}$$

is the basic length scale of the nonlinear (interface) region of the temperature profile [76, 77].

An appropriate field-theoretic model for calculating the thermal resistance is provided by model F [78, 79], confined to plate geometry with D.b.c. for ψ and supplemented by an external heat source $W_0 \sim Q$ [48, 76, 80]

$$\dot{\psi} = -2\Gamma_0 \frac{\delta H}{\delta \psi^*} + ig_0 \psi \frac{\delta H}{\delta m} + \Theta_\psi, \tag{7.8}$$

$$\dot{m} = \lambda_0 \nabla^2 \frac{\delta H}{\delta m} + g_0 \nabla j_s + W_0 + \Theta_m, \tag{7.9}$$

$$H = \int d^d x (\tfrac{1}{2}\tau_0 |\psi|^2 + \tfrac{1}{2}|\nabla\psi|^2 + \tilde{u}_0 |\psi|^4 + \tfrac{1}{2}m^2 + \gamma_0 m|\psi|^2) \tag{7.10}$$

with $j_s \equiv \mathrm{Im}\,(\psi^* \nabla\psi)$. The basic problem is to calculate the stationary-state averages $\langle \delta H/\delta m \rangle$ or $\langle j_s \rangle$ which determine the temperature profile in the cell. Similar as in statics, all nonuniversal parameters of the dynamic model (7.8)–(7.10) are known from bulk critical dynamics [27, 79], thus no further adjustment of parameters is needed in calculating the finite-size and surface properties. So far the following field-theoretic RG results are available.

(1) The (linear) bulk thermal conductivity $\lambda_T(t)$ is known up to two-loop order [27] which agrees remarkably well with recent accurate data [81, 82] up to $t = 10^{-7}$ (Fig. 16).

(2) The bulk part R_b of the Q-dependent thermal resistance for $T \gtrsim T_\lambda$ can be obtained from the temperature profile calculated in [76] up to one-loop order.

(3) The $(Q \to 0)$ Kapitza resistance $R_K(t)$ near T_λ is known [48, 80, 83] to lowest order which agrees reasonably well with the data below T_λ [84] (Fig. 17) but disagrees considerably with the existing data above T_λ [81, 82, 85] (Fig. 18). New accurate experiments above T_λ that discriminate between bulk and surface contributions would be highly desirable.

The size dependence of the measured thermal conductivity [28, 86, 87] above T_λ has also been analyzed in [87] in terms of boundary effects within an empirical model. The leading size-dependence (surface contribution) in this

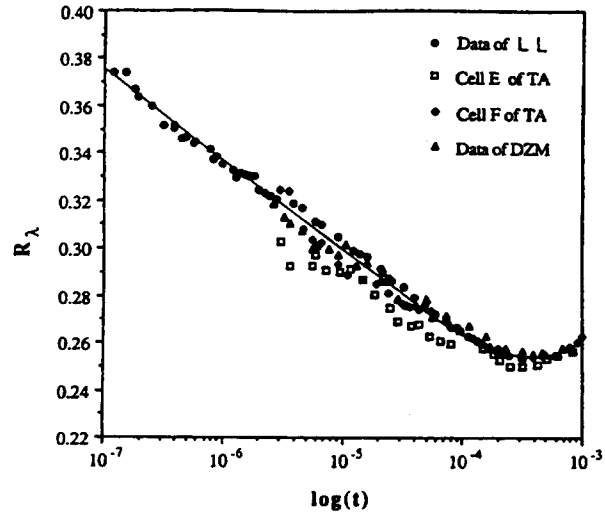

Fig. 16. Effective amplitude ratio $R_\lambda = \lambda_T g_0^{-1}[\xi k_B C_p]^{-1/2}$ *vs.* $\log_{10} t$. Theoretical prediction (solid curve) from Fig. 5(a) of [27] and from Table II of Ref. 56 quoted in [27]. Data from [81, 82] (LL), from [28] (TA) and from [91] (DZM). The non-universal increase of R_λ is due to the weak-scaling fixed point [14, 27, 88].

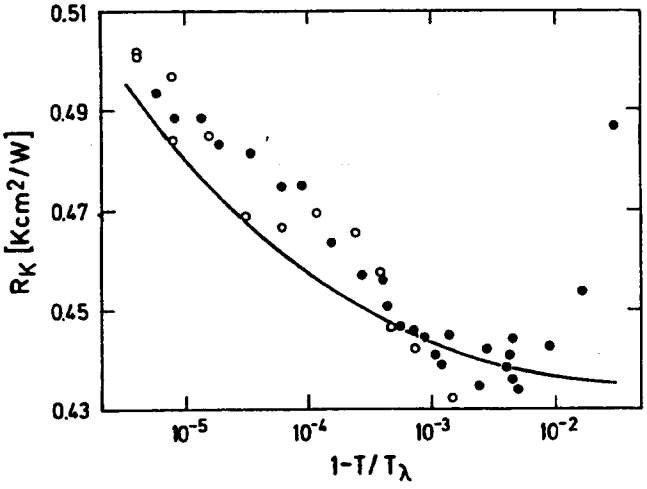

Fig. 17. Kapitza resistance R_K below T_λ. Solid line: RG theory [48, 80]. Data from [84].

analysis, however, differs from that calculated in [48, 80, 83].

A challenging task is to calculate the finite-size contribution ΔR of R and the nonlinear Q dependence of the Kapitza resistance. We expect that the resulting expression for R can be represented in a quasiscaling form, similar to that for the nonlinear temperature profile [76], where the weak-scaling fixed point [88] and the slow approach of the specific heat to its finite value at T_λ cause nonuniversal (pressure dependent) effects [27].

Measurements of the nonlinear interface profile $T_\lambda(z, Q)$ between normal-liquid and superfluid ^4He are planned for future research [89, 90]. The nonlinear Q dependence of the Kapitza resistance R_K below T_λ has already been measured [84, 91] but no theoretical explanation is available so far. Preliminary calculations [60] of the finite-size part ΔR at $Q = 0$ for cubic geometry with periodic b.c., in the spirit of the finite-size RG approach of Section 3, have indicated that this part of the problem is quite difficult because of (static and dynamic) Goldstone problems. It is conceivable that one can cope with these problems within a perturbation approach based on the decomposition (3.8) or an appropriate modification thereof. This would be a rewarding task in view of the perspective that quantitative measurements of finite-size and surface contributions to R at macroscopic distances L may become feasible under microgravity conditions [62, 82, 89, 90].

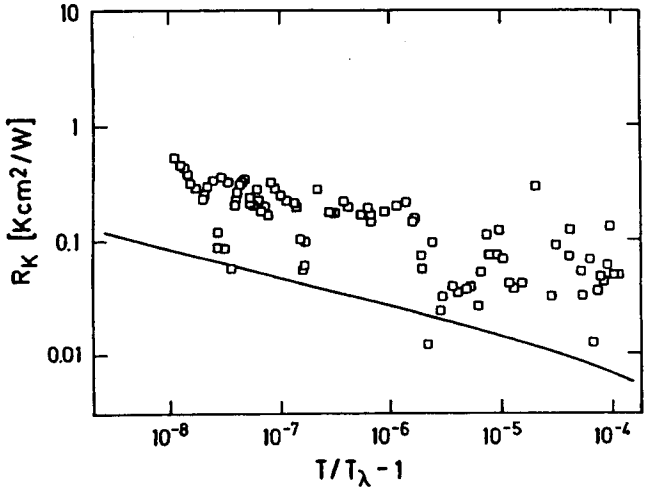

Fig. 18. Kapitza resistance R_K above T_λ. Solid line: RG theory [48]. Data from [85].

Acknowledgements

I appreciate fruitful collaboration with A. Esser, D. Frank, W. Huhn, R. Schmolke, P. Sutter and A. Wacker who have contributed substantially to the results described in this review. Support by the Sonderforschungsbereich 341 (Physik mesokopischer und niedrigdimensionaler metallischer Systeme) of the Deutsche Forschungsgemeinschaft is also acknowledged.

References

1. Fisher, M. E., in: "Critical Phenomena", Proc. 51st "Enrico Fermi" Summer School, Varenna (Edited by M. S. Green) (Academic Press, New York 1971), p. 1.
2. Suzuki, M., Progr. Theor. Phys **58**, 1142 (1977).
3. Brezin, E., J. Phys. (Paris) **43**, 15 (1982).
4. Barber, M. N., in: "Phase Transitions and Critical Phenomena" (Edited by C. Domb and J. L. Lebowitz) (Academic, New York 1983) Vol. 8, p. 145; Privman, V., in: "Finite Size Scaling and Numerical Simluation of Statistical Systems" (Edited by V. Privman) (World Scientific, Singapore 1990), p. 1; Binder, K., Annu, Rev. Phys. Chem. **43**, 33 (1992); and in: "Computational Methods in Field Theory" (Edited by H. Gausterer and C. B. Lang) (Springer, Berlin 1992), p. 59; and references therein.
5. Gasparini, F. M. and Rhee, I., in: Progr. Low Temp. Phys. XIII (Edited by D. F. Brewer) (North-Holland, Amsterdam 1992), p. 1.
6. Nissen, J. A., Chui, T. C. P. and Lipa, J. A., J. Low Temp. Phys. (1993).
7. Schmolke, R., Wacker, A., Dohm, V. and Frank, D., Physica **B165** & **166**, 575 (1990).
8. Sutter, P. and Dohm, V., Physica **B**, (1993).
9. Wacker, A. and Dohm, V., Physica **B**, (1993).
10. Chen, T.-P., Ph.D. Thesis, State University of New York, Buffalo, N.Y. (1978).
11. Chen, T.-P. and Gasparini, F. M., Phys. Rev. Lett. **40**, 331 (1978).
12. Gasparini, F. M., Chen, T.-P. and Bhattacharyya, B., Phys. Rev. **B23**, 5797 (1981).
13. Chan, M., Blum, K., Murphy, S., Wong, G. and Reppy, J. D., Phys. Rev. Lett. **61**, 1950 (1988); Wong, G. K. S., Crowell, P. A., Cho, H. A. and Reppy, J. D., Phys. Rev. Lett. **65**, 2410 (1990); Mulders, N., Mehrotra, R., Goldner, L. S. and Ahlers, G., Phys. Rev. Lett. **67**, 695 (1991); Larsen, M., Mulders, N. and Ahlers, G., Phys. Rev. Lett. **68**, 3896 (1992).
14. Dohm, V., J. Low Temp. Phys. **69**, 51 (1987); Dohm, V. and Folk, R., Physica **B109** & **110**, 1549 (1982); Hohenberg, P. C., ibid. **109** & **110**, 1436 (1982); Dohm, V. and Folk, R., in "Advances of Solid State Physics" (Edited by P. Grosse) (Vieweg, Braunschweig 1982), Vol. 22, p. 1.
15. Ginzburg, V. L. and Sobyanin, A. A., Sov. Phys. Usp. **19**, 773 (1976); Jpn. J. Appl. Phys. **26**, 1785 (1987).
16. Huhn, W. and Dohm, V., Phys. Rev. Lett. **61**, 1368 (1988).
17. Diehl, H. W., in: "Phase Transitions and Critical Phenomena" (Edited by C. Domb and J. L. Lebowitz) (Academic Press, London 1986), Vol. 10.
18. Sobyanin, A. A., Sov. Phys. JETP **36**, 941 (1973).
19. Wang, X. F., Rhee, I. and Gasparini, F. M., Physica **B165** & **166**, 593 (1990).
20. Brezin, E., Le Guillou, J. C. and Zinn-Justin, J., in: "Phase Transition and Critical Phenomena" (Edited by C. Domb and M. S. Green) (Academic Press, London 1976), Vol. 6.
21. Amit, D. J., "Field Theory, the Renormalization Group and Critical Phenomena" (World Scientific, Singapore 1978).
22. Dohm, V., Z. Phys. **B75**, 109 (1989).
23. Guo, H. and Jasnow, D., Phys. Rev. **B35**, 1846 (1987); **B39**, 753 (1989) (E).
24. Eisenriegler, E., Z. Phys. **B61**, 299 (1985).
25. Krech, M. and Dietrich, S., Phys. Rev. Lett. **66**, 345 (1991); Phys. Rev. **A46**, 1886 (1992).
26. Krech, M. and Dietrich, S., Phys. Rev. **A46**, 1922 (1992).
27. Dohm, V., Phys. Rev. **B44**, 2697 (1991), and references therein.

28. Tam, W. Y. and Ahlers, G., Phys. Rev. **B32**, 5932 (1985).
29. Hasenbusch, M. and Meyer, S., Phys. Lett. **B241**, 238 (1990).
30. Li, Y.-H. and Teitel, S., Phys. Rev. **B40**, 9122 (1989).
31. Janke, W. and Kleinert, H., in: Kleinert, H., "Gauge Fields in Condensed Matter" (World Scientific, Singapore 1989), Vol. I.
32. Wegner, F. J., Phys. Rev. **B5**, 4529 (1972).
33. Dohm, V., Esser, A. and Hermes, M., Verhandl. DPG (VI) **27**, 426 (1992); Esser, A. and Dohm, V., Verhandl. DPG (VI) **27**, 471 (1992); **28**, 749 (1993).
34. Esser, A., Diplomarbeit, Technische Hochschule Aachen (1992).
35. Esser, A. and Dohm, V., in: "The 18th IUPAP International Conference on Statistical Physics" (Edited by W. Loose) (TU Berlin 1992), p. 159.
36. Krause, J. H., Diplomarbeit, Technische Hochschule Aachen (1989).
37. Hermes, M., Diplomarbeit, Technische Hochschule Aachen (1990).
38. Gottlob, A. P., Hasenbusch, M. and Meyer, S., Verhandl. DPG (VI) **28**, 746 (1993); Nucl. Phys. B (Proc. Suppl.) **30**, 838 (1993); Gottlob, A. P. and Hasenbusch, M., preprint KL-TH-93/10, CERN-TH. 6885/93, to be published.
39. Bagnuls, C. and Bervillier, C., Phys. Rev. **B41**, 402 (1990).
40. Brezin, E. and Zinn-Justin, J., Nucl. Phys. **B257**, 867 (1985).
41. Rudnick, J., Guo, H. and Jasnow, D., J. Stat. Phys. **41**, 353 (1985).
42. Esser, A., Dohm, V. and Hermes, M., to be published.
43. Esser, A. and Dohm, V., to be published.
44. Dohm, V., Z. Phys. **B60**, 61 (1985).
45. Schloms, R. and Dohm, V., Nucl. Phys. **B328**, 639 (1989).
46. Schloms, R. and Dohm, V., Phys. Rev. **B42**, 6142 (1990).
47. O'Connor, D. and Stephens, C. R., Nucl. Phys. **B360**, 297 (1991); see also Schmeltzer, D., Phys. Rev. **B32**, 7512 (1985).
48. Frank, D. and Dohm, V., Z. Phys. **B84**, 443 (1991).
49. Wacker, A., Diplomarbeit, Technische Hochschule Aachen (1989).
50. Huhn, W., Ph.D. Thesis, Technische Hochschule Aachen (1988).
51. Rudnick, J., Gaspari, G. and Privman, V., Phys. Rev. **B32**, 7594 (1985).
52. Wacker, A. and Dohm, V., to be published.
53. Privman, V. and Fisher, M. E., J. Phys. **A16**, L295 (1983).
54. Dietrich, S. and Diehl, H. W., Z. Phys. **B43**, 315 (1981).
55. Sutter, P. and Dohm, V., to be published.
56. Goldschmidt, Y. Y. and Jasnow, D., Phys. Rev. **B29**, 3990 (1984).
57. Mikheev, L. V. and Fisher, M. E., J. Low Temp. Phys. **90**, 119 (1993).
58. Ginzburg, V. L., Piraevskii, L. P., Sov. Phys. JETP **7**, 858 (1958).
59. Schmolke, R., Diplomarbeit, Technische Hochschule Aachen (1990).
60. Frank, D., Ph.D. Thesis, Technische Hochschule Aachen (1989).
61. Pankert, J. and Dohm, V., Phys. Rev. **B40**, 10856 (1989).
62. Lipa, J. A., private communication.
63. Niemela, J. J. and Donnelly, R. J., private communication.
64. The possibility (raised in Fig. 3(b) of [26]) of a discontinuity of the bulk specific heat $C(t, \infty)$ at T_λ can be eliminated, for $\Lambda = \infty$, on the basis of Eqs. (4.14), (2.29) and (2.41) of [46]; this conclusion should remain valid also at finite Λ, thus $C(t, \infty)$ should be continuous at T_λ corresponding to $B^+ = B^- = B$.
65. Josephson, B. D., Phys. Lett. **21**, 608 (1966).
66. Hohenberg, P. C. and Martin, P. C., Ann. Phys. (N.Y.) **34**, 291 (1965).
67. Fisher, M. E., Barber, M. N. and Jasnow, D., Phys. Rev. **A8**, 1111 (1973); Rudnick, J. and Jasnow, D., Phys. Rev. **B16**, 2032 (1977).
68. Forster, D., "Hydrodynamic Fluctuations, Broken Symmetry, and Correlation Functions" (Benjamin, Reading, Mass. 1975).
69. Rhee, I., Gasparini, F. M. and Bishop, D. J., Phys. Rev. Lett. **63**, 410 (1989).
70. Privman, V., J. Phys. **A23**, L711 (1990); Physica **A177**, 241 (1991).
71. Rhee, I., Bishop, D. J. and Gasparini, F. M., Physica **B165** & **166**, 535 (1990).
72. Danchev, D., J. Stat. Phys. (1993).
73. Mon, K. K., Phys. Rev. **B44**, 2643 (1991).
74. Pollock, E. L. and Runge, K. J., Phys. Rev. **B46**, 3535 (1992).
75. Dohm, V., in: Proc. 6th Oregon Conf. on Low Temp. Phys. (Edited by R. J. Donnelly) (University of Oregon, Eugene 1989), p. 92.
76. Haussmann, R. and Dohm, V., Phys. Rev. Lett. **67**, 3404 (1991); Z. Phys. **B87**, 229 (1992).
77. Onuki, A., J. Low Temp. Phys. **50**, 433 (1983); **55**, 309 (1984).
78. Halperin, B. I., Hohenberg, P. C. and Siggia, E. D., Phys. Rev. **B13**, 1299 (1976); **B21**, 2044 (1980) (E).
79. Dohm, V., Z. Phys. **B61**, 193 (1985).
80. Frank, D. and Dohm, V., Phys. Rev. Lett. **62**, 1864 (1989).
81. Li, Q., Ph.D. Thesis, Stanford University (1991).
82. Lipa, J. A., in: Proc. 8th Oregon Conf. on Low Temp. Phys., Workshop at Washington D.C. (Edited by R. J. Donnelly) (University of Oregon, Eugene 1991), p. 130.
83. Frank, D. and Dohm, V., Physica **B165** & **166**, 543 (1990).
84. Duncan, R. V., Ahlers, G. and Steinberg, V., Phys. Rev. Lett. **58**, 377 (1987); Duncan, R. V. and Ahlers, G., Jpn. J. Appl. Phys. [Suppl.] **26-3**, 363 (1987); Phys. Rev. **B43**, 7707 (1991).
85. Li, Q., Chui, T. C. P. and Lipa, J. A., Physica **B165** & **166**, 533 (1990).
86. Lipa, J. A. and Chui, T. C. P., Phys. Rev. Lett. **58**, 1340 (1987); Chui, T. C. P., Li, Q. and Lipa, J. A., Jpn J. Appl. Phys. [Suppl.] **26-3**, 371 (1987); Lipa, J. A., Li, Q., Chui, T. C. P. and Marek, D., Nucl. Phys. B, Proc. [Suppl.] **A5**, 31 (1988).
87. Ahlers, G. and Duncan, R. V., Phys. Rev. Lett. **61**, 846 (1988).
88. De Dominicis, C. and Peliti, L., Phys. Rev. **B18**, 353 (1978).
89. Ahlers, G., J. Low Temp. Phys. **84**, 173 (1991).
90. Duncan, R. V., private communication.
91. Dingus, M., Zhong, F. and Meyer, H., J. Low Temp. Phys. **65**, 185 (1986); Zhong, F., Tuttle, J. and Meyer, H., J. Low Temp. Phys. **79**, 9 (1990).